Developing a Validated Numerical Model of Granular Material Flow in a Heat Exchanger

Samkelo M. Khumalo [1*], *Daniel M.* Madyira [1], *Waldermar F.* Cieslakiewicz [1], *Dewald* Scholtz[2], *Garikai T.* Marangwanda[1]

[1] Department of Mechanical Engineering Science, University of Johannesburg, Johannesburg, South Africa
[2] DryTech International, Johannesburg, South Africa

Abstract. This paper presents the development of a validated numerical model of granular material flowability in a heat exchanger using the DEM modelling in STAR-CCM+ software. The model is developed based on an experiment. The simulation model is validated qualitatively and quantitatively from experimental data. The comparison between the experimental and simulated velocities, velocity profiles and mass flowrates demonstrate a high degree of similarity. For instance, the percentage difference of mass flowrate between the experiment and simulation data is 5.61% and the maximum percentage difference of the particle velocity is 9.53% which reflects a reasonable level of agreement.

1. Introduction

Baumgarten et al. [1] define granular material as a collection of aggregates comprising many discrete and disconnected particles. They are ubiquitous in industrial and natural processes [1], with numerous applications ranging from pharmaceutical industries [2] to geological engineering [3]. The behaviour of granular materials, particularly their flowability, plays an important role in industrial processes such as storage, transportation, mixing, heating, and drying [4]. Understanding and predicting the flowability of granular materials in hoppers is essential for optimizing hopper design and ensuring smooth operation [5].

Numerous experimental studies have traditionally been used to investigate granular flow, providing valuable insights into flow patterns [6], discharge rates [7], and velocity profiles [8], just to mention a few. However, experimental approaches can be time-consuming, expensive, and limiting when it comes to capturing the detailed dynamics of particles and their interactions. A numerical simulation based on the Discrete Element Method (DEM) is one of the most widely used tools for studying granular materials. As stated by Balevičius et al. [9], DEM provides a detailed understanding of granular material behaviour, including the positions, velocities, and accelerations of individual particles, as well as the interparticle forces acting between them. This method allows granular material to be modelled as an assembly of particles while easily tracking each particle's dynamic parameters such as velocity, position, acceleration, and orientation.

Balevičius et al. [9] and Balevičius et al. [10] studied the discharge flow of granular materials in inclined wall and vertical wall hoppers with the same outlet size. In their studies, they observed that inclined wall hoppers are characterized by higher mass flow rates compared to vertical-walled hoppers; however, they did not address the effects of friction factors on granular flowability. Sun et al. [11] investigated the effects of wall friction on mass discharge rates in vertically walled hoppers with eccentric outlets. They observed that when the friction coefficient is high, a greater portion of the particles' gravitational potential energy is dissipated through rotational motion due to resistance, thereby decreasing the mass flow rate.

Despite these findings, granular material flowability in hoppers remains complex and challenging for predictive modelling because of factors such as frictional forces, bulk density variations, and particle interactions. As stated by Shi et al. [12], the Hertz–Mindlin (also known as the no-slip) contact model serves as a default contact model in DEM modelling. This model accurately and efficiently calculates the contact forces between particles and their surroundings [12]. The model comprises normal and tangential forces [13], which need to be accurately determined through experiments for more realistic simulations. For DEM analysis, the main Hertz–Mindlin parameters are [14]:

- Normal restitution coefficient
- Tangential restitution coefficient
- Coefficient of rolling resistance
- Static friction coefficient

* Corresponding author: samkelok746@gmail.com

The aim of this study is to develop a numerical model that can be used to predict granular flowability in a heat exchanger (also known as an inclined wall hopper or space wedge hopper). The study will validate the simulated results against experimental data and determine the factors affecting flowability. By integrating DEM simulations and experimental observations, this study aims to provide a better understanding of granular flowability in heat exchangers, thereby contributing to the design optimization of these devices.

2 Numerical Analysis of Granular Material Flow in Heat Exchanger

2.1. Material Modelling

The material under study is silicon, with properties given in Table 1. The values presented in Table 1 are used as reference values and have been obtained through experimental measurements and literature studies. Based on DEM studies that use materials similar to silicon, different restitution coefficients have been assumed and used. For instance, Qin et al. [15] assume a restitution coefficient of 0.77, Jian et al. [16] and Staron et al. [17] assume 0.50, while Grima et al. [18] assume 0.55. Using these values as references through a trial-and-error approach, the restitution coefficient was narrowed down to 0.50.

Table 1. Parameters of silicon granules used for the simulation [19].

Parameter	Value
Particle diameter (mm)	4
Density (kg/m³)	2329
Young's modulus (GPa)	112
Poisson's ratio	0.28
Static friction coefficient	0.268
Coefficient of rolling resistance	0.001
Tangential restitution coefficient	0.5
Normal restitution coefficient	0.5

2.2. Geometrical Modelling

The heat exchanger model has an overall length of 430 mm, a depth of 80 mm, a width of 200 mm, and an outlet opening of 8.8 mm. The cylindrical holes in the geometry represent the heating elements. Figure 1a shows the heat exchanger geometry. In STAR-CCM+, DEM does not require mesh sensitivity analysis as long as the mesh size is larger than the particle size [14]. For this reason, a polyhedral mesher and surface remesher with an element size of 10 mm were used, generating 35,480 polyhedral cells. Figure 1b shows the meshed geometry.

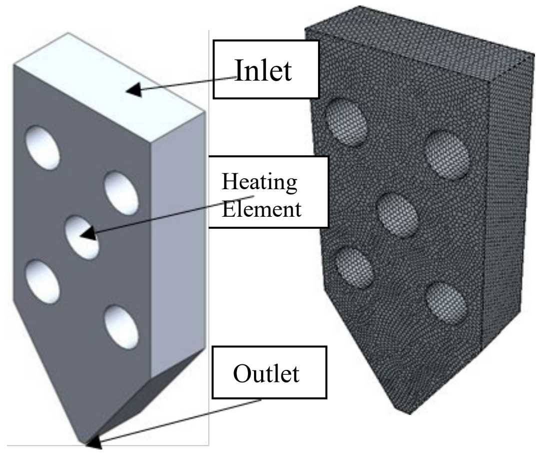

(a) (b)

Fig 1. Heat exchanger geometry: (a) isometric view; (b) mesh analysis**.**

2.3. Boundary Conditions

The boundary conditions were selected to replicate the experimental conditions. Particle–wall interactions were defined using a friction coefficient of 0.25, a restitution coefficient of 0.5, and zero surface roughness to imitate the smooth walls of stainless steel. Particles were introduced at the top of the heat exchanger with a uniform velocity of 0.5 m/s to provide an initial velocity, while the outlet was set to allow particles to discharge freely under gravity. Gravity was set to 9.81 m/s² in the negative vertical direction.

2.4. Physics Continuum

A physics continuum consists of multiple physics models, such as material models, selected flow solvers, and other applicable models. Each continuum represents a single material that occupies the entire domain it defines [14]. For this simulation, the main physics models required within the continuum include segregated flow, implicit unsteady formulation, Lagrangian multiphase, DEM, multiphase interaction, and constant density [14].

2.5. Simulation Results

Particles are injected into the heat exchanger through the inlet while the outlet remains closed. Figure 2 shows the filling process, with Figure 2a representing the initial filling stage (t = 0.15 s) and Figure 2b representing the fully filled stage (t > 1.2 s). Once the geometry is fully filled, as shown in Figure 2b, the total number of retained particles is 94,650. The outlet is then opened to allow particles to flow out under the influence of gravity.

Once a stable flow condition is achieved, the particle flow profile is presented in Figure 3. Particles shown in red indicate higher velocities exceeding 9 mm/s, whereas particles shown in blue represent slower flow velocities approaching 0 mm/s.

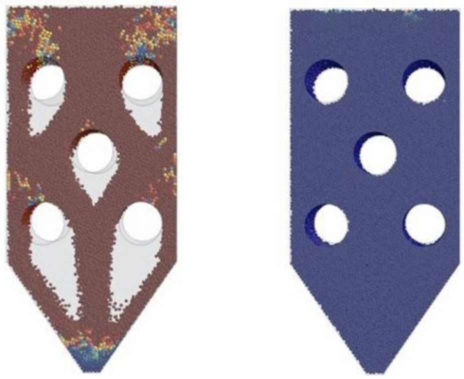

(a) **(b)**

Fig 2. Particles filling the geometry: (a) initial filling stage; (b) fully filled stage.

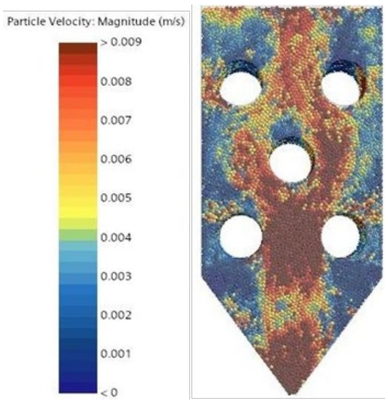

Fig 3. Particle flow velocity profile.

As expected, particles flow faster toward the centre of the heat exchanger and slower toward the walls due to particle blockages between the heating elements and the side walls. Additionally, the particle mass flow rate was measured and plotted against time, as shown in Figure 4. Using the averaging method, the mass flow rate was determined to be 133.16 g/s, as indicated by the average particle mass flow rate in Fig 4.

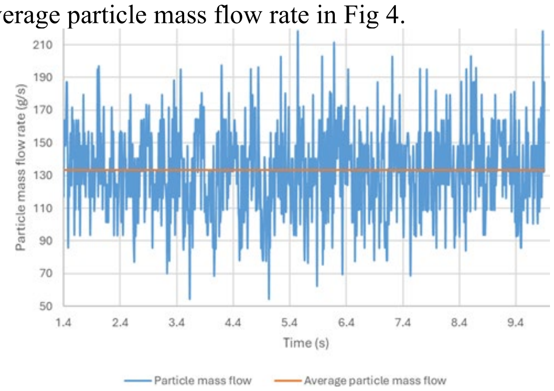

Fig 4. Particle mass flow rate over a period of 10 seconds.

3. Model Validation

The comparison of particle flow velocities between the simulation and the experiment, as shown in Figure 5, demonstrates a high degree of similarity. It is evident that particle velocity is not uniform within the heat exchanger. Higher flow velocities are observed at the centre of the heat exchanger, as indicated by the particles shown in red in the simulation model (Figure 5a) and by the particles shown in green in the experimental results (Figure 5b). Figure 5 indicates that the simulation model effectively captures the key dynamics of particle flow within the heat exchanger.

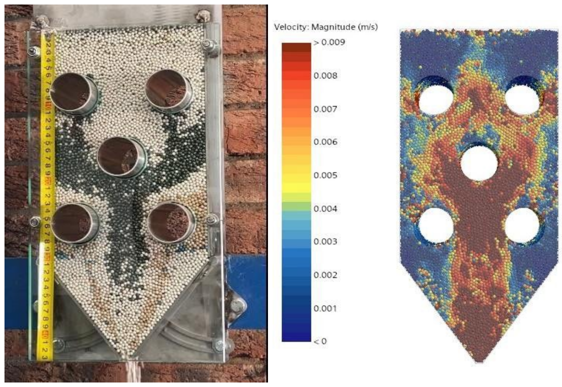

(a) **(b)**

Fig 5. Particle flow velocity comparison between: (a) experimental; (b) simulation data.

Using the same approach for identifying particle velocities as in the experimental analysis, different regions were selected and labelled, as shown in **Fig**. 6 The average velocities in these regions were recorded and are presented in Table 2 for both experimental measurements and numerical simulations.

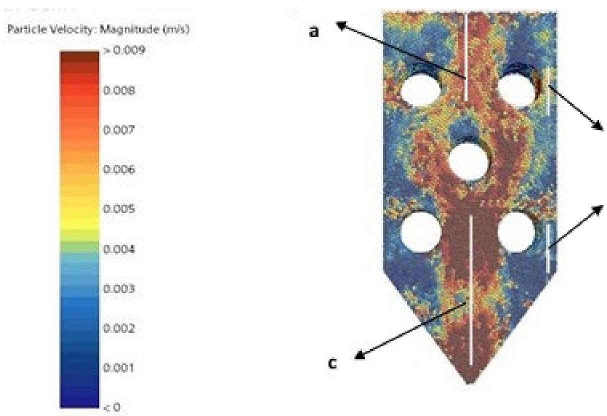

Fig.6. Particle velocity at different regions.

Table 2. Particle velocity comparison in different regions between experimental and simulation data.

Area	Experimental velocity (mm/s)	Simulation velocity (mm/s)	Percentage difference (%)
a	6.83	6.50	4.95
b	5.47	5.50	0.55
c	9.09	10.00	9.53
d	1.63	1.50	8.31

4. Discussion

As expected, Region C exhibits the highest particle velocities, exceeding 9 mm/s. This behaviour is attributed to particles near the centre of the outlet having a direct path to exit, thereby experiencing less resistance compared to particles near the walls. These findings are consistent with the velocity profiles obtained both experimentally and numerically, as shown in Fig 5.

The highest percentage difference between the experimental and simulation velocity results is 9.53%, which reflects a good level of agreement, considering unavoidable experimental measurement errors and modelling assumptions inherent in numerical simulations. Similarly, the mass flow rate of granular materials was measured as 140.85 g/s experimentally and 133.16 g/s in the simulation, resulting in a percentage difference of 5.61%.

Furthermore, the number of particles calculated experimentally—assuming a particle packing density of 63%—was 95,413, while the simulation yielded 94,650 particles. This corresponds to a percentage difference of only 0.8%, further demonstrating the robustness and accuracy of the numerical model.

5. Conclusions

Using experimental values as reference points, the granular flow within the heat exchanger was successfully simulated to closely replicate real-world operating conditions. The Hertz–Mindlin contact model proved to be an effective and reliable approach for DEM analysis, particularly when frictional parameters are carefully determined using experimental data and supporting literature.

The results demonstrate that particles at the centre of the heat exchanger flow faster than those closer to the walls, confirming non-uniform velocity distributions. The percentage difference between experimental and simulated mass flow rates was 5.61%, while the maximum percentage difference in particle velocity was 9.53%. These results validate the accuracy of the numerical model and establish its reliability for further analytical studies.

Consequently, the developed simulation framework can be considered reliable for analysing particle dynamics in heat exchanger geometries and may serve as a useful tool for design optimization and performance evaluation.

Funding

This research was funded by the University of Johannesburg and DryTech International.

References

1. A. S. Baumgarten, J. Moreno, B. Kuwik, S. Ghosh, R. Hurley, and K. T. Ramesh, A predictive model for fluid-saturated, brittle granular materials during high-velocity impact events, J. Mech. Phys. Solids, **187**, 105644, (2024).
2. I. Wünsch, J. H. Finke, E. John, M. Juhnke, and A. Kwade, A mathematical approach to consider solid compressibility in the compression of pharmaceutical powders, Pharmaceutics, **11**(3), 1–19, (2019).
3. H. Ding et al., Particle breakage and its mechanical response in granular soils: A review and prospect, Constr. Build. Mater., **409**, 133948, (2023).
4. K. Traina, R. Cloots, S. Bontempi, G. Lumay, N. Vandewalle, and F. Boschini, Flow abilities of powders and granular materials evidenced from dynamical tap density measurement, Powder Technol., **235**, 842–846, (2013).
5. X. Huang, Q. Zheng, D. Liu, A. Yu, and W. Yan, A design method of hopper shape optimisation with improved mass flow pattern and reduced particle segregation, Chem. Eng. Sci., **253**, 117579, (2022).
6. R. M. Gandia, F. C. Gomes, W. C. de Paula, and P. J. A. Rodriguez, The influence of flow pattern and hopper angle on static and dynamic pressures in slender silos, Powder Technol., **427**, 1, (2023).
7. Y. Xiao, Y. Han, F. Jia, H. Liu, G. Li, P. Chen, X. Meng, and S. Bai, Experimental study of granular flow transition near the outlet in a flat-bottomed silo, Biosyst. Eng., **202**, 16–27, (2021).
8. S. Tong, B. Miao, M. Shen, G. Zhang, and S. H. Chan, Experimental and numerical analysis of granular phase flow behaviour in a rotary bed reactor: Velocity profile study, Powder Technol., **444**, 119992, (2024).
9. R. Balevičius, R. Kačianauskas, R. Mróz, and I. Z. Sielamowicz, Analysis and DEM simulation of granular material flow patterns in hopper models of different shapes, Adv. Powder Technol., **22**, 226–235, (2011).
10. R. Balevičius, R. Kačianauskas, Z. Mróz, and I. Sielamowicz, Discrete element method applied to multi-objective optimisation of discharge flow

parameters in hoppers, Struct. Multidiscip. Optim., **31**, 163–175, (2006).

11. Mu and H. Yang, Mass discharge rate of granular flow in eccentric silos with variable side wall friction, Powder Technol., **449**, 120438, (2025).
12. J. Shi, Z. Shan, and H. Yang, Research on the macro- and meso-mechanical properties of frozen sand mould based on Hertz–Mindlin with bonding model, Particuology, **88**, 176–191, (2024).
13. R. D. Mindlin and H. Deresiewicz, Elastic spheres in contact under varying oblique forces, J. Appl. Mech., **20**(3), 327–344, (1953).
14. Siemens Digital Industries Software, Simcenter STAR-CCM+ User Guide, Siemens, (2023).
15. R. Qin, H. Fang, F. Liu, D. Xing, J. Yang, N. Lv, J. Chen, and J. Li, Study on physical and contact parameters of limestone by DEM, IOP Conf. Ser.: Earth Environ. Sci., **252**, 5, (2019).
16. H. Jiang, J. Nie, O. C. Debanath, and Y. Li, Dynamic column collapse of dry granular materials with multi-scale shape characteristics, Comput. Geotech., **177**, 106873, (2025).
17. L. Staron and E. J. Hinch, The spreading of a granular mass: Role of grain properties and initial conditions, Granul. Matter, **9**(3–4), 205–217, (2007).
18. A. P. Grima and P. W. Wypych, Development and validation of calibration methods for discrete element modelling, Granul. Matter, **13**(2), 127–132, (2011).
19. B. M. Barkachary and S. N. Joshi, Finite element simulation of single point diamond turning of silicon, Proc. Int. Conf. Precis. Meso Micro Nano Eng. (COPEN-8), 1023–1026, (2013).